

1 **Title page**

2 **Effect of rTMS on cerebral functional hierarchical structure in**
3 **schizophrenia**

4 Hanxi Wu¹, Hechun Li^{1,2*}, Kewei Xiong¹, Sisi Jiang^{1,3,4}, Huan Huang¹, Changyue Hou¹, Jingyu
5 Zhou¹, Roberto Rodriguez-Labrada⁵, Dezhong Yao^{1,3,4}, Cheng Luo^{1,3,4*}

6 ¹ The Clinical Hospital of Chengdu Brain Science Institute, School of Life Science and Technology,
7 University of Electronic Science and Technology of China, Chengdu, 610054, P. R. China.

8 ² The school of Sport Training, Chengdu Sport University, Chengdu, 610041, P. R. China

9 ³ Research Unit of NeuroInformation, Chinese Academy of Medical Sciences, 2019RU035,
10 Chengdu, 610054, P. R. China

11 ⁴ China-Cuba Belt and Road Joint Laboratory on Neurotechnology and Brain-Apparatus
12 Communication, University of Electronic Science and Technology of China, Chengdu, 610054, P. R.
13 China

14 ⁵ Cuban Neuroscience Center, La Habana, Cuba

15
16 * Corresponding authors: hechun_li@foxmail.com (Hechun Li); chengluo@uestc.edu.cn (Cheng
17 Luo).

18

19

20 Abstract

21 **Background** The hierarchical functional structure reflects the process of integrating primary
22 information to form higher-order cognition in the human brain. Schizophrenia, as a severe chronic
23 psychiatric illness, has been demonstrated to exhibit an abnormal cerebral functional hierarchical
24 structure. Although repetitive transcranial magnetic stimulation (rTMS) of the dorsolateral prefrontal
25 cortex (DLPFC) has shown therapeutic efficacy on schizophrenia, the mechanism of rTMS in
26 schizophrenia is still unclear. Thus, this study attempted to reveal the modulation of rTMS on the
27 cerebral functional hierarchy and its potential molecular mechanism in schizophrenia.

28 **Methods** A longitudinal study was performed on 53 patients with schizophrenia (randomly assigned
29 to the rTMS group or drug treatment group). Additionally, 24 age- and gender-matched healthy adults
30 were recruited. Functional gradient analysis was executed to depict the hierarchical organization of
31 schizophrenia. The alteration of the functional gradients at baseline and after 4 weeks of treatment was
32 evaluated in schizophrenia to detect the effect of rTMS on the cerebral hierarchical structure.

33 **Results** We found rTMS alleviated the compression of the fronto-parietal network, the core node of
34 the salience network (SN), and the bilateral middle temporal areas in schizophrenia. Leveraging human
35 brain gene expression data, we identified a spatial correlation between the expression of schizophrenia-
36 related genes and impaired functional gradients, and further revealed a close association of the
37 modulatory effects of rTMS with pathways related to neuroplasticity and neuroimmune processes.
38 Furthermore, the alterations of gradient induced by rTMS were associated with the alleviation of
39 clinical symptoms in schizophrenia, suggesting that the altered hierarchical structure may play an
40 important role in the treatment of schizophrenia.

41 **Conclusions** Our findings indicate that the alteration of cerebral hierarchy induced by rTMS
42 contributes to clinical symptom improvement in schizophrenia and provides new evidence for the
43 efficacy of rTMS in the treatment of schizophrenia.

44 **Keywords:** schizophrenia, rTMS, hierarchical structure, functional gradient analysis, gene
45 expression

46

47 **Introduction**

48 Schizophrenia is a severe chronic mental disorder characterized by multisensory integration deficits
49 (Postmes et al. 2014). Currently, the clinical treatment of patients with schizophrenia mainly relies on
50 antipsychotic drugs. Antipsychotics usually provide good relief from positive symptoms but have little
51 effect on the cognitive deficits and negative symptoms (Hsu et al. 2018; Kay et al. 1987). Meanwhile,
52 non-invasive brain stimulation, especially repetitive transcranial magnetic stimulation (rTMS), has
53 been widely adopted as adjunctive therapy to improve clinical symptoms in schizophrenia (Sciortino
54 et al. 2021). Accumulating evidence suggests that this technique has significant therapeutic potential
55 in the clinical treatment of schizophrenia (Lefaucheur et al. 2020; Sale et al. 2015; Sciortino et al.
56 2021). For example, several studies have found that high-frequency rTMS (HF-rTMS) applied to the
57 left DLPFC can significantly improve the negative symptoms of schizophrenia (Gan et al. 2021; Li et
58 al. 2016). A meta-analysis also showed that rTMS on the left DLPFC with a total of pulses < 30,000
59 was more effective in improving working memory than pulses \geq 30,000 (Jiang et al. 2019). However,
60 the mechanisms underlying the effect of TMS on the improvement of schizophrenia symptoms remains
61 unclear. Numerous studies found that rTMS can modulate local neural activity and functional
62 connectivity between the brain regions as well as induce effects that spread across networks (Beynel
63 et al. 2020; Chen et al. 2013), and improve the clinical symptoms (Gromann et al. 2012; Han et al.
64 2023; Sultana et al. 2023). For instance, a study using an activating TMS sequence (triplet at 10 Hz)
65 over the left Brodmann area 9 resulted in a local “spill-over” in activation to neighboring ipsilateral
66 regions (Webler et al. 2020). Thus, the rTMS may modulate both local and long-range functional
67 connectivity of key brain regions to achieve therapeutic effects in schizophrenia.

68 The principle that brain functional topography plays a critical role in cognition is increasingly
69 supported by evidence from neuroimaging (Huntenburg et al. 2018), microstructural differentiation
70 (Beul et al. 2019; Paquola et al. 2019), transcriptomics (Hansen et al. 2021) and electrophysiology
71 (Murray et al. 2014; Thomas Yeo et al. 2011). The cerebral hierarchical structure facilitates the
72 integration of multimodal information from the primary sensorimotor system (Holmes et al. 2023;
73 Mesulam 1998), and is helpful for high-order systems to process abstract cognitive information.

74 Functional gradient analysis is a powerful tool for revealing the abnormal hierarchical structure in
75 neurological and psychotic disorders (Margulies et al. 2016; Vafaii et al. 2024). For example, the
76 principal gradient in major depressive disorder showed lower gradient scores in default mode network
77 (DMN) but higher scores mainly in the visual and sensorimotor cortices compared with the control
78 group (Xia et al. 2022). Our previous studies proposed a framework to elucidate the interaction
79 between low- and high-level functional abnormalities within cerebellar and cerebellar-cerebral cortical
80 circuits in schizophrenia (Dong et al. 2019, 2022). These results reflect the impairment of hierarchical
81 processing in mental disorders (Fornito et al. 2012; Holmes et al. 2023; Kebets et al. 2019; Zhang et
82 al. 2023) and demonstrate that functional gradient may serve as a neuroimaging biomarker to identify
83 the altered hierarchical processing in brain disorders. Despite these findings, little is known about the
84 relationship between the genetic basis underlying brain functional gradients and their modulation by
85 rTMS in schizophrenia.

86 Schizophrenia is characterized by high heritability and multiple genetic variations (Owen et al. 2016;
87 Singh et al. 2022). A study using cell-resolution data from a standardized in situ hybridization (ISH)
88 platform identified 67 risk loci for schizophrenia (Zeng et al. 2012). A previous study has shown that
89 abnormalities in the morphological similarity network of patients with schizophrenia are significantly
90 correlated with the expression patterns of schizophrenia-related genes (Morgan et al. 2019). Thus, the
91 convergent expression of these schizophrenia-associated loci in neurons and their disruption of
92 neuronal functionality may also underlie aberrations in brain functional hierarchical structure. The
93 Allen Human Brain Atlas (AHBA) microarray dataset has provided an anatomically comprehensive
94 transcriptomic map of the human brain (Hawrylycz et al. 2012; Sunkin et al. 2012). Concurrently,
95 integrated imaging-transcriptomic analyses have uncovered potential biological pathways underlying
96 regional brain alterations across multiple psychiatric disorders (Ardesch et al. 2023; Jiang et al. 2023;
97 Li et al. 2021). Such cross-scale approaches offer a powerful framework to investigate how
98 schizophrenia-associated microscale changes contribute to aberrant macroscale functional hierarchies.

99 Hence, to further understand the mechanism of rTMS in schizophrenia, we aimed to utilize the
100 functional gradient analysis to investigate the effects of rTMS on the organization of hierarchical
101 structure and to further explore the relationship with genetic factors. Here, we hypothesized that the

102 abnormalities in the brain functional hierarchy in schizophrenia may result from certain genetic factors,
103 and rTMS could modulate the cerebral hierarchical structure to alleviate the clinical symptoms of
104 schizophrenia. To verify this hypothesis, first, the functional gradient analysis was applied to the
105 longitudinal data acquired before and after rTMS treatment to explore the modulation of HF-rTMS on
106 the brain functional hierarchy organization in schizophrenia and its relationship with changes in
107 clinical symptoms in this study. The first three functional gradient patterns were analyzed to reveal the
108 altered hierarchical structure induced by HF-rTMS. Second, we assessed the relationship between the
109 changes in these gradients and clinical symptom response in schizophrenia. Third, we established the
110 relationship between abnormal functional hierarchies in schizophrenia and gene expression patterns.
111 Finally, we performed enrichment analyses to identify the biological pathways related to alterations in
112 functional hierarchies.

113 **Materials and methods**

114 **Participants**

115 In this study, 59 patients with schizophrenia as the experimental group and 24 age- and gender-
116 matched healthy subjects as the control group (HC group) were recruited from the Clinical Hospital of
117 Chengdu Brain Science Institute, UESTC, China. Psychiatric symptom severity of all patients was
118 evaluated using the Positive and Negative Syndrome Scale (PANSS). The inclusion criteria for the
119 schizophrenia subjects were as follows: 1) meeting the ICD-10 diagnostic criteria for schizophrenia;
120 2) having no obvious organic brain lesions; 3) the negative symptom sub-score of PANSS ≥ 21 and
121 the positive symptom subscale-score of PANSS ≤ 24 ; 4) the absence of distinct auditory hallucinations
122 or a history of other mental disorders; 5) having no drug abuse or suicidal tendencies; 6) having no
123 neurological disorders in patients or their first-degree relatives; 7) having no contraindications to TMS
124 or MRI. The detailed demographic information was described in supplementary materials (Table.S1)
125 and our previous research (Huang et al. 2022). This study was carried out in accordance with the
126 Declaration of Helsinki, and was reviewed and approved by the Ethics Committee of the Clinical
127 Hospital of Chengdu Brain Science Institute (No. 106142021030920). All participants and/or their

128 guardians were conscious of the purpose and procedure of this study and signed written informed
129 consent. The clinical trial number: ChiCTR2100049273.

130 **Experimental design**

131 The patients were randomly divided into two groups. The group that received both HF-rTMS
132 treatment and a stable dosage of antipsychotics was designated the TMS stimulation group (TSZ
133 group), while the group that only received antipsychotic medication was designated the drug group
134 (DSZ group). Due to excessive head motion or failure to complete the experiment, 6 patients (3 patients
135 in the TSZ group and 3 patients in the DSZ group) were excluded from the analysis. Therefore, 27
136 patients in the TSZ group and 26 patients in the DSZ group were included in the subsequent analysis.
137 There were no significant differences between the two groups in age, gender, years of education, illness
138 duration, or antipsychotic equivalent. For the TSZ group, HF-rTMS was administered using a
139 YRDCCY-1 stimulator (Yiruide Medical Equipment New Technology Co., Ltd., Wuhan, China) with
140 a figure-of-8 coil (B9076). The coil was positioned tangentially to the plane of the skull to provide
141 stimulation, and the junction of the two loops was aligned with the stimulation target. In the period of
142 treatment, 27 patients in the TSZ group received five sessions of HF-rTMS treatment per week for 4
143 weeks. The TMS coil was positioned on the F3 (a reference to the 10-20 EEG system), corresponding
144 to the left DLPFC (Jiang et al. 2019; Shi et al. 2014). Each session delivered 1000 pulses/day (a total
145 of 20 sets of pulse trains, each with 50 pulses, 5s per train, and an interval of 30s) at 10-Hz and an
146 intensity of 110% of resting motor threshold. MRI scanning and PANSS assessments were conducted
147 at baseline and post-treatment. All patients maintained the same stable medication throughout the study.

148 **MRI data acquisition and pre-processing**

149 MRI data were acquired on a 3-Tesla MRI scanner (GE DISCOVERY MR750) with an eight-
150 channel phased-array head coil at the University of Electronic Science and Technology of China
151 (UESTC). The resting-state fMRI data were acquired using a standard gradient-echo echo-planar
152 imaging (EPI) sequence with the following parameters: repetition time(TR) = 2000 ms, echo time(TE)
153 = 30 ms, flip angle(FA) = 90°, matrix size = 64 × 64, field of view(FOV) = 240 × 240 mm², slice
154 thickness = 4 mm (gap = 0.4 mm), voxel size = 3.75 × 3.75 × 4.00 mm³, and 35 axial slices in each

155 volume. The scan duration was 510 seconds, which yielded 255 whole-brain volumes. The high-
156 resolution T1-weighted images were acquired using a three-dimensional fast spoiled gradient echo
157 sequence. The parameters were as follows: TR = 6.008 ms, TE = 1.984 ms, FA = 9°, matrix size = 256
158 × 256, FOV = 25.6 × 25.6 cm², slice thickness = 1 mm (no gap). A total of 152 slices were acquired
159 for each subject. During scanning, participants were instructed to remain still and be relaxed with their
160 eyes while fixating on a cross on the screen, and their heads were immobilized with foam padding to
161 minimize the effects of movement.

162 The preprocessing of fMRI data was carried out using the data processing and analysis for (resting-
163 state) brain imaging (DPABI) software package (Yan et al. 2016), including: 1) the first 5 time points
164 discarded due to the inhomogeneity of the magnetic field; 2) slice timing correction; 3) motion
165 correction; 4) realignment; 5) normalization and resampled the voxel size into 5 × 5 × 5 mm³; 6) regressed
166 out nuisance signals (including white matter (WM), cerebrospinal fluid (CSF), linear trend, global
167 signal (GS), 24 head motion parameters (6 motion parameters (three translations and three rotations),
168 and their first-order derivatives, and the squared terms of these 12 parameters); 7) band-pass filtered
169 between 0.01-0.1 Hz.

170 **Functional gradient and spatial dispersion analyses**

171 In this study, we performed diffusion map embedding to identify the functional gradients for each
172 participant. This nonlinear dimensionality reduction technique captures gradual transitions in
173 functional connectivity patterns across the cortex by mapping high-dimensional similarity data into a
174 low-dimensional space. It more effectively projects both local and long-distance connections into a
175 common space compared to linear approaches (Margulies et al. 2016). The resultant components of
176 this data-driven analysis are functional gradients that describe the connectome where each voxel is
177 located along a gradient according to its connectivity pattern (Dong et al. 2022). Gradient values are
178 unitless; higher or lower scores reflect the relative similarity changes in functional connectivity
179 patterns in each dimension.

180 To investigate alterations in functional hierarchy as represented by functional gradients in
181 schizophrenia, we computed the voxel-wise functional connectivity (of the cerebral cortex) for each

182 individual. Subsequently, we performed threshold processing on the connectivity matrix, retaining the
183 top 10% of positive connectivity in each row. Cosine similarity was calculated to generate the
184 individual affinity matrix, which served as the input of the diffusion embedding map. This algorithm
185 identifies low-dimensional gradient component, ordering them by the proportion of variance explained.
186 Each gradient was aligned to the group-level gradient component template, which was generated from
187 an average connectivity matrix of the HC group. Since the first three gradients accounted for the vast
188 majority of data variation, subsequent analysis focused on these three gradients.

189 Furthermore, to quantify the whole-brain connectivity separation captured by the multi-dimensional
190 gradients, we calculated gradient eccentricity, a measure representing the 3D gradient dispersion
191 property (Park et al. 2021). Gradient eccentricity was calculated as the Euclidean distance between the
192 centroid of all vertices extracted from the HC template and all vertices in each 3D gradient point.
193 Group-level differences in gradient eccentricity was then examined in the following statistical analysis
194 to evaluate the effect of TMS on gradient dispersion.

195 **Statistical analysis**

196 First, to evaluate alteration in hierarchical functional topography in schizophrenia, we detected the
197 difference in the principal gradient between the schizophrenia group at baseline and the HCs using the
198 two-sample t-test (age and gender as the covariates). Then, the repeated measure analysis of variance
199 (rANOVA) (between-group factor: treatment (TMS + Drug vs. only Drug), within-group factor: time
200 (baseline vs. post-treatment)) was performed to investigate the effects of TMS on the principal gradient
201 to the third gradient, controlling the age and gender. The post hoc tests were conducted using a two-
202 sample t-test (between-group) or paired t-test (within-group).

203 Then, to identify the association between the altered brain functional gradient induced by the HF-
204 rTMS and clinical symptom improvement in schizophrenia, we further examined the relationship
205 between the altered gradients (post-treatment minus baseline) within regions showing significant
206 interaction effects and the changes in PANSS scores (baseline minus post-treatment) by Spearman
207 correlation. The significance of these correlations was assessed using permutation testing (5,000
208 permutations). Specifically, a null distribution was generated by randomly shuffling the pairing

209 between gradient values and PANSS scores across participants 5,000 times, recalculating the
210 correlation coefficient each time. The observed correlation was then compared against this null
211 distribution to obtain a permutation p-value (p_{perm}). The PANSS difference was calculated as (baseline
212 minus post-treatment) so that a positive value indicated a reduction in symptoms (i.e., improvement).

213 In addition, to evaluate the influence of global signal regression (GSR), we also performed
214 functional gradient analysis based on functional connectivity without global signal regression (without
215 GSR).

216 **Gene expression related to functional hierarchy**

217 The AHBA dataset (<http://human.brain-map.org>) provides publicly available normalized gene
218 expression data derived from bulk microarray analysis of tissue samples obtained from six healthy
219 adult human donors. More than 20,000 genes across 3,702 brain regions in MRI-derived stereotactic
220 space are provided. In present analysis, considering that the AHBA dataset contains only two right
221 hemisphere data, only the left hemisphere was used. Following the preprocessing pipeline described
222 by Arnatkevic et al., we assigned samples to Brainnetome atlas (210 cortical subregions) (Fan et al.
223 2016). Then we obtained the estimated expression values for each of the genes in regions of the left
224 hemisphere, resulting in a regional transcription matrix (105 regions \times 10,027 gene expression levels).
225 More detailed steps for regional gene expression estimation are described in our previous
226 research (Jiang et al. 2023). Next, to investigate gene expression associated with changes in brain
227 functional hierarchy in patients with schizophrenia, partial least squares (PLS) analysis was performed
228 separately on the patients versus healthy controls statistical map and the post-treatment versus pre-
229 treatment statistical map in patients receiving TMS treatment. In each the PLS regression model, the
230 left hemisphere T-statistic map served as the response variable, and the transcriptional activity data of
231 10027 genes served as the predictor variables. This yielded two distinct gene expression-weighted
232 brain maps: one related to functional impairment and the other associated with TMS modulation effects.
233 For the correlation between the first component of PLS (PLS1) and T-statistical maps, spin tests based
234 on spherical rotations (5,000 iterations) was employed to eliminate spatial autocorrelation (Alexander-
235 Bloch et al. 2018). And bootstrap method was used to estimate the variability of each gene's PLS1

236 weights, which resamples cortical regions with replacement. Then the weight of each gene was
237 transformed to a Z-score reflecting the contribution of each gene to PLS1 by calculating the ratio of
238 its weight to its bootstrap standard error. Based on the Z-score value, we ranked the genes and selected
239 genes that significantly contributed to changes in brain functional hierarchy ($p < 0.005$, false discovery
240 rate [FDR]-corrected).

241 In addition, to investigate the transcriptional correlation between disease-related gene and
242 alterations in brain functional hierarchy, we overlapped the 10,027 background genes with 67
243 schizophrenia-related genes previously defined within the AHBA dataset. This dataset provides large-
244 scale, cellular-resolution spatial expression patterns of 1,000 genes profiled using ISH (Zeng et al.
245 2012). Then, we estimated the associations between these 52 overlapped genes and gradient statistical
246 maps using Spatial Spearman's correlation ($p_{\text{spin}} < 0.05$, FDR corrected).

247 **Enrichment analysis**

248 Enrichment analyses were performed to further explore the molecular functions, cellular
249 components, or biological processes implicated in the hierarchical changes of brain function in patients.
250 Genes with higher loadings in the PLS1- and PLS1+ gene lists were selected for the enrichment
251 analysis using Metascape website (<https://metascape.org/gp/index.html#/main/step1>). We conducted
252 gene enrichment analyses on the results of the two PLS analyses respectively. For the genes related to
253 baseline functional impairment, we selected 1748 PLS1+($Z > 5$) genes and 658 PLS1-($Z < -5$) genes as
254 the input for the enrichment analysis. Similarly, for the genes related to the TMS modulation effect,
255 considering that the therapeutic effect of the four-week TMS treatment is relatively mild, we selected
256 the 23 PLS1+ and 2,989 PLS1- weighted genes (all $p_{\text{FDR}} < 0.005$) as the input for the enrichment
257 analysis.

258 **Results**

259 **The effect of rTMS on the gradients of schizophrenia**

260 Consistent with previous research (Margulies et al. 2016), the two ends of the principal gradient
261 (referred to as gradient 1) corresponded to the sensorimotor cortex and the DMN. The two ends of the

262 second gradient (gradient 2) are the visual cortex and sensorimotor cortex. Besides, the third gradient
263 (gradient 3) extends from the sensorimotor and the DMN to the fronto-parietal network (FPN) (Fig.1A,
264 1B; Supplementary Fig.S1). Similar distribution patterns were observed in gradients without GSR
265 (Supplementary Fig.S2, Fig.S3). In addition, compared with the HC group, patients with schizophrenia
266 showed an increased principal gradient in bilateral sensorimotor cortices (Fig.2A; Supplementary
267 Fig.S4A).

268 For the principal gradient, a significant interaction between rTMS treatment and time was observed
269 ($p < 0.05$) (Fig.2B), involving the occipital lobe, the left inferior frontal gyrus, the left middle frontal
270 gyrus, the superior frontal gyrus, and subcortical regions. Compared to the baseline condition, paired
271 t-test revealed that rTMS significantly increased principal gradient values in the left DLPFC, left insula,
272 and left inferior parietal lobule (IPL), while resulting in decreased principal gradient in the bilateral
273 MT and frontoparietal regions (Fig.2C, 2D). For gradient 2, significant interaction effects were
274 identified primarily in the occipital lobe, middle temporal gyrus and right inferior frontal gyrus. The
275 paired t-test between post- and baseline showed a significant increase in the right superior temporal
276 gyrus and right Heschl gyrus, and a decrease in the left inferior occipital gyrus (Supplementary Fig.S5).
277 The rANOVA of the gradient 3 indicated significant interaction effects in the bilateral angular gyrus,
278 the bilateral IPL, the right middle frontal gyrus, and the middle cingulate gyrus (Fig.3A). Compared
279 to baseline, the paired t-test results revealed consistent increases in gradient 3 values across most of
280 these areas (Fig.3B, 3C). Similar findings were observed in gradients without GSR (Supplementary
281 Fig.S4B, S4C, S6, S7).

282 Additionally, we calculated the eccentricity of the three gradient components for each of the
283 individuals. The results showed that the regions of increased eccentricity after rTMS treatment were
284 mainly located in bilateral IPL (Supplementary Fig.S8).

285 **Correlations between altered functional gradients and clinical variables**

286 We extracted gradient scores from 9 regions of interest (ROIs) that showed significant interaction
287 effects in both the principal gradient and the third gradient to examine the relationship between the
288 altered functional gradients and clinical scale (PANSS positive, negative, general psychopathology

289 subscales and total scores). An increase in the principal gradient within the left insula induced by rTMS
290 was significantly associated with the improvement of positive symptoms ($r=0.401$, $p_{\text{perm}}=0.035$)
291 (Fig.4A). A decreased in the principal gradient within the left middle temporal area induced by TMS
292 was significantly associated with improvement of general psychopathology symptoms ($r=-0.489$,
293 $p_{\text{perm}}=0.011$) (Fig 4B). The results of the permutation tests are provided in Supplementary Fig. S9.

294 **Correlations between altered functional gradients and genetic factors**

295 To explore the contribution of the schizophrenia-related genes to alterations of functional hierarchy,
296 we first obtained the overlapped genes from the 67 schizophrenia-related genes identified by ISH and
297 10,027 background genes. The complete list of overlapping genes is provided in supplementary
298 materials (Table.S2). Sixteen of the 52 overlapping schizophrenia-associated genes showed significant
299 correlations with changes in principal gradient ($p < 0.05$, FDR corrected) (Fig 5A). Six genes exhibited
300 significant positive correlation (i.e., *ATF4*: $r = 0.58$, $p_{\text{spin}} = 0.003$; *NRG1*: $r = 0.55$, $p_{\text{spin}} = 0.005$; *PCNT*:
301 $r = 0.46$, $p_{\text{spin}} = 0.037$; *PVALB*: $r = 0.57$, $p_{\text{spin}} = 0.008$; *FEZ1*: $r = 0.47$, $p_{\text{spin}} = 0.001$; *NDE1*: $r = 0.39$,
302 $p_{\text{spin}} = 0.005$). Ten genes exhibited significant negative correlation (i.e., *BDNF*: $r = -0.56$, $p_{\text{spin}} < 0.001$;
303 *GRIN2B*: $r = -0.51$, $p_{\text{spin}} = 0.001$; *GRM7*: $r = -0.39$, $p_{\text{spin}} = 0.035$; *HTR2C*: $r = -0.53$, $p_{\text{spin}} = 0.006$;
304 *KCNN3*: $r = -0.51$, $p_{\text{spin}} = 0.001$; *PRODH*: $r = -0.42$, $p_{\text{spin}} < 0.001$; *SYN2*: $r = -0.58$, $p_{\text{spin}} < 0.001$;
305 *PDLIM5*: $r = -0.38$, $p_{\text{spin}} = 0.014$; *NPAS3*: $r = -0.44$, $p_{\text{spin}} = 0.005$; *PPP1R1B*: $r = -0.40$, $p_{\text{spin}} = 0.006$).

306 We performed two sets of PLS regressions to identify the spatial patterns of gene expression that
307 were associated with the alteration of functional hierarchy in patients with schizophrenia. Subsequently,
308 enrichment analyses were conducted separately for the lists of significantly expressed genes derived
309 from each PLS regression analyses.

310 In the first PLS regression analysis, we investigated the correlation between gene expression and
311 the principal gradient abnormalities in schizophrenia (Fig.5). The PLS1 explained 48.6% of the
312 variance in the principal gradient abnormality (i.e., T-map comparing patients at baseline to the HC
313 group). PLS1 gene expression weights were significantly positively correlated with the principal
314 gradient T-map (Fig 5D, $r = 0.70$, $p_{\text{spin}} < 0.0001$). Then we converted the PLS1 scores to Z-scores and
315 ranked the normalized PLS loadings (Fig.5E, $p_{\text{FDR}} < 0.005$). We found 1,748 PLS1+($Z > 5$) positively

316 weighted gene expressions were over-expressed as increased principal gradient value and 659 PLS1-
317 ($Z < -5$) negatively weighted gene expressions were under-expressed as decreased principal gradient
318 value (all $p_{FDR} < 0.005$). Next, we aligned the Gene Ontology (GO), Kyoto Encyclopedia of Genes and
319 Genomes (KEGG) and Reactome (R-HAS) pathways with the above total 2,047 genes list. The
320 enriched terms of top twenty significant pathways are shown in Fig 5F, which included seventeen GO
321 biological processes, one KEGG pathway and two R-HSA pathways.

322 In the second PLS regression, we examined the correlation between gene expression and the
323 principal gradient improvement induced by rTMS (Fig.6). The PLS1 explained 23.1% of the variance
324 in the principal gradient improvement (i.e., T-map comparing the TSZ group at post-rTMS to baseline).
325 PLS1 gene expression weights were significantly positively correlated with the principal gradient T-
326 map (Fig.6C, $r = 0.48$, $p_{spin} = 0.0035$). Similarly, we ranked the normalized weights of PLS1 scores
327 (Fig.6D, $p_{FDR} < 0.005$). We found 288 PLS1- ($Z < -5$) negatively weighted gene expressions were
328 under-expressed as decreased principal gradient value, but no PLS1+ ($Z > 5$) positive weighted gene
329 was observed. Given the relatively modest association between the short-term effects of rTMS and
330 gene expression, we included 23 PLS1+ and 2,989 PLS1- weighted genes (all $p_{FDR} < 0.005$) in the
331 enrichment analysis. The enriched terms of top twenty significant pathways are shown in Fig.6E,
332 comprising sixteen GO biological processes, one KEGG pathway and three R-HSA pathways.

333 Discussion

334 This study utilized functional gradient analyses to explore the effects of HF-rTMS on functional
335 hierarchical organization structure in patients with schizophrenia, and systematically compared the
336 abnormal enriched pathways in schizophrenia as well as the biological pathway remodeling that
337 accompanied the gradient reversal after rTMS treatment. The alleviated compression by rTMS mainly
338 located in the FPN region (increased gradient scores in the prefrontal lobe, the top of the sensorimotor-
339 to-association axis) and the visual network (decreased gradient scores in the occipital lobe, the bottom
340 of the sensorimotor-to-association axis) in principal gradient. Meanwhile, the alteration of gradient
341 scores was associated with the relief of clinical symptom. These findings suggest that HF-rTMS might
342 relieve the clinical symptoms of schizophrenia to some degree by relieving the suppressed brain

343 hierarchical structure. This supports the view that the reduction of separation of the primary
344 sensorimotor cortex from the higher-order cortex disrupts the macroscale network hierarchy
345 organization in schizophrenia. Interestingly, this compression was alleviated by rTMS combined with
346 medication rather than only drugs, highlighting the specific role of rTMS in modulating brain
347 hierarchical organization.

348 The functional connectivity gradient mapping method provides a simplified representation of brain
349 function in the lower-order to higher-order cognitive regions(Katsumi et al. 2023), which can reflect
350 the macroscopic changes in the cortical hierarchy of schizophrenia. In both the HC and schizophrenia
351 groups, the principal gradient depicted an axis extending from primary sensory areas (visual and
352 sensorimotor) to the DMN, gradient 2 depicted an axis extending from visual to sensorimotor cortices,
353 and gradient 3 depicted an axis extending from sensorimotor and DMN to the FPN. This pattern
354 confirms that gradient analysis robustly captures the brain's hierarchical organization. Nonetheless,
355 we observed a compressed principal gradient in schizophrenia, which is consistent with our previous
356 studies(Dong et al. 2020). Together, these results indicate the cerebral functional hierarchical structure
357 has been disrupted in schizophrenia although the inherent hierarchy is retained.

358 In our study, the regulatory effect of rTMS on functional connectivity gradient in schizophrenia was
359 obvious. The DLPFC is the core hub of FPN (Menon et al. 2022). Extensive evidence indicates that
360 rTMS targeted in the left DLPFC can alter the functional connectivity between DLPFC and other
361 regions (Bation et al. 2021; Eldaief et al. 2011), which supported the excitement of targeted regions
362 can modulate its distributed network connections. The rTMS targeted in the left DLPFC has shown
363 beneficial effects on symptoms such as auditory verbal hallucinations, cognitive deficits, and
364 schizophrenia, and has been associated with improvements in working memory (De Weijer et al. 2014;
365 Hasan et al. 2016; Liu et al. 2025; Ragland et al. 2004). Our previous study found that the FC temporal
366 variability between the DLPFC (target) and regions in the cortical-thalamic-cerebellar circuit is
367 significantly reduced after HF-rTMS intervention (Huang et al. 2022). In this current study, the
368 increased gradient scores in the left DLPFC reflected the changed hierarchical organization of the
369 target region after rTMS treatment, and this shift may further help improve the abnormal cognitive
370 control function of FPN in schizophrenia.

371 Although few studies have focused on the effect of rTMS on brain hierarchical structure, the
372 previous studies demonstrated that the rTMS not only can modulate the functional connectivity of
373 target regions but also can change the remote regions (Wang et al. 2024). The rTMS could also change
374 the graph property of connectivity (Li et al. 2024; Olejarczyk et al. 2020), suggesting that the rTMS
375 could reshape the whole brain organization. Mounting studies indicates that cognitive deficits in
376 schizophrenia are related to abnormal mutual communication between networks. A dynamic causal
377 modeling analysis has found that the cross-network interactions centered at salience network (SN) are
378 most significantly reduced, and that dysregulation of triple-network interaction aggravates clinical
379 symptoms in schizophrenia (Supekar et al. 2019; Xi et al. 2021). In this study, rTMS-induced increases
380 in the principal gradient were observed in the left insula, which is a core area of SN acting as a switch
381 to convert internally oriented cognition to externally oriented attention through activation of either the
382 DMN or central executive network (Uddin 2015; Zhao et al. 2022). This change was associated with
383 improvement in clinical symptoms. The insula-anchored SN plays a central role in the aberrant
384 mapping of salient external and internal events in schizophrenia (Menon et al. 2023). This is consistent
385 with the consensus that SN can activate the FPN to maximize attention to the task (Schimmelpfennig
386 et al. 2023). From a theoretical perspective, increased functional hierarchy and enhanced function
387 integration of the SN induced by rTMS could help identify relevant stimuli within a continuous stream
388 of sensory input, which in turn could contribute to more efficient functional switching of the FPN in
389 the triple-network framework and improving the clinical symptom in schizophrenia. However, this
390 speculation should be further examined in future studies.

391 In addition, the altered functional gradient was also found in MT. As a highly specialized visual area,
392 research on MT has focused on its role in visual information processing. The local information of the
393 primary visual cortex (area striata, V1) must be integrated across a wider space and time into a global
394 concept via high-order motion mechanisms in area V5 (i.e. middle temporal area, MT) in the dorsal
395 pathway (Born et al. 2005; Tadin et al. 2011; Urbaniak et al. 2024). Studies have consistently revealed
396 deficits in performance on multiple information-integration related tasks specific to the high-order
397 motion area V5 in patients with schizophrenia, such as distinguishing stimuli of different velocities
398 figure-ground segregation, and temporal order judgment (Kandil et al. 2013). Similar to these studies,

399 the principal gradient level of MT in schizophrenics showed a compression which represented a
400 reduced degree of separation of primary sensory processing from the associated cortex. After four
401 weeks of HF-rTMS treatment, this compression pattern was alleviated, and the change correlated with
402 improvement in the general pathological symptoms of schizophrenia. Given the limited prior research
403 on rTMS-induced modulation of MT, we propose that HF-rTMS might restore the bottom-up
404 transmission of sensory information in the dorsal information pathway with MT as the hub by adjusting
405 the functional connectivity gradient in the MT region. Moreover, HF-rTMS targeted left DLPFC might
406 also modulate the top-down cognitive pathway, which further improved the inefficient integration
407 between the two pathways to alleviate clinical symptoms. Together, these observations reinforce the
408 importance of studying the abnormal information flow between primary sensorimotor and high-order
409 association cortices in schizophrenia.

410 Among the correlations of overlapped schizophrenia-related genes, the expression of the *ATF4* gene
411 and the *SYN2* gene respectively showed the strongest positive and negative correlations with the
412 functional gradient changes. Oxidative stress is a convergence point for schizophrenia genetic and
413 environmental risk factors (Cuenod et al. 2022), while *ATF4* is a key transcription factor in integrating
414 stress responses (Costa-Mattioli et al. 2020). *ATF4* also affects trafficking of GABA_B receptors, which
415 in turn modulates the excitability properties of neurons (Corona et al. 2018). In addition, the *SYN2*
416 gene has been reported to confer susceptibility to schizophrenia (Lee et al. 2005), and its abnormal
417 expression in emotional disorders is highly associated with decreased DNA methylation (Cruceanu et
418 al. 2016). Together with prior evidence on schizophrenia risk genes, our findings further support a
419 genetic basis for the disorder. Besides, we identified the weighted combination of genes that
420 significantly co-localized with functional gradient changes. Of the 16 overlapped schizophrenia-
421 related genes correlated with functional gradient abnormalities in patients, two distinct patterns
422 emerged regarding rTMS treatment response. Six genes with positive weights on PLS1 for the disease
423 abnormality showed negative weights for the post-rTMS improvement. Conversely, the ten genes with
424 negative weights for the disease abnormality showed no significant weighted contribution to the
425 improvement. This divergence suggests that rTMS might primarily modulate genetic mechanisms
426 governed by genes that are positively associated with the functional hierarchy aberrations in

427 schizophrenia (i.e., *ATF4*, *NRG1*, *PCNT*, *PVALB*, *FEZ1*, *NDE1*).

428 Furthermore, enrichment analysis identified the biological pathways that were highly associated
429 with the alteration of functional hierarchy in schizophrenia. These pathways showed pronounced
430 enrichment in biological pathways associated with ion homeostasis and transmembrane transport
431 mechanisms, and cellular metabolic activities. These results are highly consistent with the classical
432 hypothesis that schizophrenia is a disorder of neurotransmitter dysregulation (Eyles 2021; Howes et
433 al. 2009). The patient group showed enrichment in multiple neurophysiological processes, suggesting
434 that the abnormality of the brain's functional gradient stems not only from functional decoupling, but
435 also from underlying molecular and cellular defects. The findings suggest that abnormal synaptic
436 function, disorder in the integration of neuronal networks, and systemic metabolic imbalance together
437 constitute the cross-scale circuit abnormalities which influenced cognitive and perceptual symptoms
438 in schizophrenia. It is worth noting that after receiving rTMS treatment, patients showed significant
439 enrichment of pathways related to neuroplasticity regulation, including “cell morphogenesis”,
440 “microtubule cytoskeleton organization”, and “actin filament-based processes”. This indicates that
441 rTMS may partially reverse the neural connectivity abnormalities by promoting neuronal structural
442 reorganization and synaptic plasticity — a perspective supported by animal studies (Cirillo et al. 2017;
443 Hoogendam et al. 2010). In particular, the *Rho GTPase* is a regulatory factor that plays a crucial role
444 in maintaining metabolic homeostasis (Møller et al. 2019). The enrichment of *Rho GTPase* signaling
445 pathway further supports that rTMS may affect the function of neural network by regulating the
446 dynamics of cytoskeleton and signal transduction pathway (Sharbafshaaer et al. 2024). Furthermore,
447 the neuroinflammation hypothesis has recently gained considerable attention in the field of psychiatric
448 disorders (Melnikov et al. 2025). This study provides evidence supporting this hypothesis: the
449 enrichment of pathways such as “response to oxidative stress” and “cellular response to cytokine
450 stimulus” after treatment suggests that rTMS may exert its therapeutic effects by modulating
451 neuroimmune mechanisms.

452 **Limitations**

453 There are several limitations associated with our study. First, the sample size of the current study

454 was relatively small, and future studies with larger cohorts are warranted. Second, although a drug
455 control group was set up, our study lacked a sham TMS control group, which may confuse our results
456 with a degree of placebo effect. Third, the stimulation target was based on a standardized location
457 rather than individualized neuronavigation. Fourth, the use of left hemispheric transcriptomic data
458 limited the generalizability of our spatial correlation analyses to whole-brain patterns. Despite these
459 limitations, this study provides novel evidence linking alterations in cerebral functional hierarchical
460 structure and clinical improvement following HF-rTMS to underlying gene expression patterns in
461 schizophrenia.

462 **Conclusion**

463 Overall, this study demonstrates that HF-rTMS targeted left DLPFC combined with drug treatment
464 can improve the clinical symptoms in patients with schizophrenia. This improvement is linked to the
465 alleviation of abnormal compression pattern of functional hierarchy, as captured by the first three
466 gradients of brain functional connectivity. The concrete manifestation is the regulation of the hierarchy
467 of SN and FPN that may enhance their interaction and transmission of attention information. Our
468 findings indicate that the mechanism by which rTMS ameliorates abnormal brain functional hierarchy
469 in schizophrenia involves multiple biological processes such as ion transport, cellular metabolic and
470 immune responses. The present study provides experimental evidence supporting the clinical validity
471 of HF-rTMS therapy. This would be a necessary work to focus on the patterns of hierarchy variation
472 between these specific brain regions of schizophrenia to promote the exploration of biomarker-
473 potential of functional gradients and clarify the mechanisms of rTMS therapy. Future research should
474 employ longitudinal designs to track gradient changes, thereby further verifying how TMS effects
475 propagate through the cortical hierarchy in patients with schizophrenia.

476 **Author contributions**

477 **Conceptualization:** Hanxi Wu, Hechun Li, Cheng Luo. **Methodology:** Hanxi Wu, Hechun Li,
478 Jingyu Zhou, Roberto Rodriguez-Labrada, Sisi Jiang. **Data curation:** Kewei Xiong, Huan Huang,
479 Changyue Hou. **Formal analysis:** Hanxi Wu. **Visualization:** Hanxi Wu, Kewei Xiong. **Software:**

480 Hechun Li. **Writing-Original draft preparation:** Hanxi Wu, Hechun Li, Sisi Jiang, Dezhong Yao,
481 Cheng Luo. **Supervision:** Sisi Jiang, Cheng Luo. **Funding acquisition:** Cheng Luo.

482 **Conflicts of interest**

483 The authors declare that they have no known competing financial interests or personal relationships
484 that could have appeared to influence the work reported in this paper. All authors have approved the
485 final manuscript.

486 **Acknowledgment and funding**

487 We are grateful to all the participants in this study. This work was supported by National Key R&D
488 Program of China, (2024YFE0215100), the STI 2030-Major Projects (2022ZD0208500), the National
489 Nature Science Foundation of China (62401124, 62201133 and 82371560), the CAMS Innovation
490 Fund for Medical Sciences (CIFMS) (No.2019-I2M-5-039), Project of Science and Technology
491 Department of Sichuan Province (23NSFSC0016), and the Fundamental Research Funds for the
492 Central Universities (ZYGX2022YGRH017), the grant from Chengdu Science and Technology
493 Bureau(2024-YF05-02056-SN).

494 **Data and code availability statement**

495 The code of gradient analysis is openly available from the BrainSpace toolbox: <http://brainspace.readthedocs.io>. The data are not publicly available due to privacy or ethical restrictions. Sharing and
497 re-use of data need the expressed written permission of the authors and clearance from the relevant
498 institutional review.

499 **References**

500 Alexander-Bloch, Aaron F., Shou, Haochang, Liu, Siyuan, et al. (2018) On testing for spatial
501 correspondence between maps of human brain structure and function. *NeuroImage* **178**
502 <https://doi.org/10.1016/j.neuroimage.2018.05.070>

503 Ardesch, Dirk Jan, Libedinsky, Ilan, Scholtens, Lianne H., et al. (2023) Convergence of brain

- 504 transcriptomic and neuroimaging patterns in schizophrenia, bipolar disorder, autism spectrum
505 disorder, and major depressive disorder. *Biological Psychiatry: Cognitive Neuroscience and*
506 *Neuroimaging* **8**:6. <https://doi.org/10.1016/j.bpsc.2022.12.013>
- 507 Bation, Rémy, Magnin, Charline, Poulet, Emmanuel, et al. (2021) Intermittent theta burst
508 stimulation for negative symptoms of schizophrenia—A double-blind, sham-controlled pilot
509 study. *Npj Schizophrenia* **7**:1. <https://doi.org/10.1038/s41537-021-00138-3>
- 510 Beul, Sarah F., and Hilgetag, Claus C. (2019) Neuron density fundamentally relates to
511 architecture and connectivity of the primate cerebral cortex. *NeuroImage* **189**
512 <https://doi.org/10.1016/j.neuroimage.2019.01.010>
- 513 Beynel, Lysianne, Powers, John Paul, and Appelbaum, Lawrence Gregory (2020) Effects of
514 repetitive transcranial magnetic stimulation on resting-state connectivity: A systematic review.
515 *NeuroImage* **211** <https://doi.org/10.1016/j.neuroimage.2020.116596>
- 516 Born, Richard T., and Bradley, David C. (2005) STRUCTURE AND FUNCTION OF
517 VISUAL AREA MT. *Annual Review of Neuroscience* **28**:1.
518 <https://doi.org/10.1146/annurev.neuro.26.041002.131052>
- 519 Chen, Ashley C., Oathes, Desmond J., Chang, Catie, et al. (2013) Causal interactions
520 between fronto-parietal central executive and default-mode networks in humans. *Proceedings*
521 *of the National Academy of Sciences* **110**:49. <https://doi.org/10.1073/pnas.1311772110>
- 522 Cirillo, G., Di Pino, G., Capone, F., et al. (2017) Neurobiological after-effects of non-
523 invasive brain stimulation. *Brain Stimulation* **10**:1. <https://doi.org/10.1016/j.brs.2016.11.009>
- 524 Corona, Carlo, Pasini, Silvia, Liu, Jin, et al. (2018) Activating transcription factor 4 (ATF4)
525 regulates neuronal activity by controlling GABA_B R trafficking. *The Journal of Neuroscience*
526 **38**:27. <https://doi.org/10.1523/JNEUROSCI.3350-17.2018>
- 527 Costa-Mattioli, Mauro, and Walter, Peter (2020) The integrated stress response: From
528 mechanism to disease. *Science* **368**:6489. <https://doi.org/10.1126/science.aat5314>
- 529 Cruceanu, Cristiana, Kutsarova, Elena, Chen, Elizabeth S., et al. (2016) DNA
530 hypomethylation of synapsin II CpG islands associates with increased gene expression in
531 bipolar disorder and major depression. *BMC Psychiatry* **16**:1. <https://doi.org/10.1186/s12888-016-0989-0>
- 533 Cuenod, Michel, Steullet, Pascal, Cabungcal, Jan-Harry, et al. (2022) Caught in vicious
534 circles: A perspective on dynamic feed-forward loops driving oxidative stress in schizophrenia.
535 *Molecular Psychiatry* **27**:4. <https://doi.org/10.1038/s41380-021-01374-w>
- 536 De Weijer, Antoin D., Sommer, Iris E.C., Lotte Meijering, Anne, et al. (2014) High frequency
537 rTMS; a more effective treatment for auditory verbal hallucinations?. *Psychiatry Research*:

- 538 *Neuroimaging* **224**:3. <https://doi.org/10.1016/j.psychresns.2014.10.007>
- 539 Dong, Debo, Duan, Mingjun, Wang, Yulin, et al. (2019) Reconfiguration of Dynamic
540 Functional Connectivity in Sensory and Perceptual System in Schizophrenia. *Cerebral Cortex*
541 **29**:8. <https://doi.org/10.1093/cercor/bhy232>
- 542 Dong, Debo, Luo, Cheng, Guell, Xavier, et al. (2020) Compression of Cerebellar Functional
543 Gradients in Schizophrenia. *Schizophrenia Bulletin* **46**:5.
544 <https://doi.org/10.1093/schbul/sbaa016>
- 545 Dong, Debo, Guell, Xavier, Genon, Sarah, et al. (2022) Linking cerebellar functional
546 gradients to transdiagnostic behavioral dimensions of psychopathology. *NeuroImage: Clinical*
547 **36** <https://doi.org/10.1016/j.nicl.2022.103176>
- 548 Eldaief, Mark C., Halko, Mark A., Buckner, Randy L., et al. (2011) Transcranial magnetic
549 stimulation modulates the brain's intrinsic activity in a frequency-dependent manner.
550 *Proceedings of the National Academy of Sciences* **108**:52.
551 <https://doi.org/10.1073/pnas.1113103109>
- 552 Eyles, Darryl W. (2021) How do established developmental risk-factors for schizophrenia
553 change the way the brain develops?. *Translational Psychiatry* **11**:1.
554 <https://doi.org/10.1038/s41398-021-01273-2>
- 555 Fan, Lingzhong, Li, Hai, Zhuo, Junjie, et al. (2016) The Human Brainnetome Atlas: A New
556 Brain Atlas Based on Connectional Architecture. *Cerebral Cortex* **26**:8.
557 <https://doi.org/10.1093/cercor/bhw157>
- 558 Fornito, Alex, Zalesky, Andrew, Pantelis, Christos, et al. (2012) Schizophrenia,
559 neuroimaging and connectomics. *NeuroImage* **62**:4.
560 <https://doi.org/10.1016/j.neuroimage.2011.12.090>
- 561 Gan, Hong, Zhu, Junjuan, Zhuo, Kaiming, et al. (2021) High frequency repetitive
562 transcranial magnetic stimulation of dorsomedial prefrontal cortex for negative symptoms in
563 patients with schizophrenia: A double-blind, randomized controlled trial. *Psychiatry Research*
564 **299** <https://doi.org/10.1016/j.psychres.2021.113876>
- 565 Gromann, Paula M., Tracy, Derek K., Giampietro, Vincent, et al. (2012) Examining
566 frontotemporal connectivity and rTMS in healthy controls: Implications for auditory
567 hallucinations in schizophrenia. *Neuropsychology* **26**:1. <https://doi.org/10.1037/a0026603>
- 568 Han, Xiaowei, Zhu, Zhengyang, Luan, Jixin, et al. (2023) Effects of repetitive transcranial
569 magnetic stimulation and their underlying neural mechanisms evaluated with magnetic
570 resonance imaging-based brain connectivity network analyses. *European Journal of Radiology*
571 *Open* **10** <https://doi.org/10.1016/j.ejro.2023.100495>

- 572 Hansen, Justine Y., Markello, Ross D., Vogel, Jacob W., et al. (2021) Mapping gene
573 transcription and neurocognition across human neocortex. *Nature Human Behaviour* **5**:9.
574 <https://doi.org/10.1038/s41562-021-01082-z>
- 575 Hasan, Alkomiet, Guse, Birgit, Cordes, Joachim, et al. (2016) Cognitive Effects of High-
576 Frequency rTMS in Schizophrenia Patients With Predominant Negative Symptoms: Results
577 From a Multicenter Randomized Sham-Controlled Trial. *Schizophrenia Bulletin* **42**:3.
578 <https://doi.org/10.1093/schbul/sbv142>
- 579 Hawrylycz, Michael J., Lein, Ed S., Guillozet-Bongaarts, Angela L., et al. (2012) An
580 anatomically comprehensive atlas of the adult human brain transcriptome. *Nature* **489**:7416.
581 <https://doi.org/10.1038/nature11405>
- 582 Holmes, Alexander, Levi, Priscila T., Chen, Yu-Chi, et al. (2023) Disruptions of Hierarchical
583 Cortical Organization in Early Psychosis and Schizophrenia. *Biological Psychiatry: Cognitive
584 Neuroscience and Neuroimaging* **8**:12. <https://doi.org/10.1016/j.bpsc.2023.08.008>
- 585 Hoogendam, Janna Marie, Ramakers, Geert M.J., and Di Lazzaro, Vincenzo (2010)
586 Physiology of repetitive transcranial magnetic stimulation of the human brain. *Brain
587 Stimulation* **3**:2. <https://doi.org/10.1016/j.brs.2009.10.005>
- 588 Howes, O. D., and Kapur, S. (2009) The dopamine hypothesis of schizophrenia: Version III-
589 the final common pathway. *Schizophrenia Bulletin* **35**:3.
590 <https://doi.org/10.1093/schbul/sbp006>
- 591 Hsu, Wen-Yu, Lane, Hsien-Yuan, and Lin, Chieh-Hsin (2018) Medications Used for
592 Cognitive Enhancement in Patients With Schizophrenia, Bipolar Disorder, Alzheimer's
593 Disease, and Parkinson's Disease. *Frontiers in Psychiatry* **9**
594 <https://doi.org/10.3389/fpsy.2018.00091>
- 595 Huang, Huan, Zhang, Bei, Mi, Li, et al. (2022) Reconfiguration of Functional Dynamics in
596 Cortico-Thalamo-Cerebellar Circuit in Schizophrenia Following High-Frequency Repeated
597 Transcranial Magnetic Stimulation. *Frontiers in Human Neuroscience* **16**
598 <https://doi.org/10.3389/fnhum.2022.928315>
- 599 Huntenburg, Julia M., Bazin, Pierre-Louis, and Margulies, Daniel S. (2018) Large-Scale
600 Gradients in Human Cortical Organization. *Trends in Cognitive Sciences* **22**:1.
601 <https://doi.org/10.1016/j.tics.2017.11.002>
- 602 Jiang, Yi, Guo, Zhiwei, Xing, Guoqiang, et al. (2019) Effects of High-Frequency
603 Transcranial Magnetic Stimulation for Cognitive Deficit in Schizophrenia: A Meta-Analysis.
604 *Frontiers in Psychiatry* **10** <https://doi.org/10.3389/fpsy.2019.00135>
- 605 Jiang, Sisi, Huang, Huan, Zhou, Jingyu, et al. (2023) Progressive trajectories of
606 schizophrenia across symptoms, genes, and the brain. *BMC Medicine* **21**:1.

- 607 <https://doi.org/10.1186/s12916-023-02935-2>
- 608 Kandil, Farid I., Pedersen, Anya, Wehnes, Jana, et al. (2013) High-level, but not low-level,
609 motion perception is impaired in patients with schizophrenia. *Neuropsychology* **27**:1.
610 <https://doi.org/10.1037/a0031300>
- 611 Katsumi, Yuta, Zhang, Jiahe, Chen, Danlei, et al. (2023) Correspondence of functional
612 connectivity gradients across human isocortex, cerebellum, and hippocampus.
613 *Communications Biology* **6**:1. <https://doi.org/10.1038/s42003-023-04796-0>
- 614 Kay, S. R., Fiszbein, A., and Opler, L. A. (1987) The Positive and Negative Syndrome Scale
615 (PANSS) for Schizophrenia. *Schizophrenia Bulletin* **13**:2.
616 <https://doi.org/10.1093/schbul/13.2.261>
- 617 Kebets, Valeria, Holmes, Avram J., Orban, Csaba, et al. (2019) Somatosensory-Motor
618 Dysconnectivity Spans Multiple Transdiagnostic Dimensions of Psychopathology. *Biological*
619 *Psychiatry* **86**:10. <https://doi.org/10.1016/j.biopsych.2019.06.013>
- 620 Lee, Hee Jae, Song, Ji Young, Kim, Jong Woo, et al. (2005) Association study of
621 polymorphisms in synaptic vesicle-associated genes, SYN2 and CPLX2, with schizophrenia.
622 *Behavioral and Brain Functions* **1**:1. <https://doi.org/10.1186/1744-9081-1-15>
- 623 Lefaucheur, Jean-Pascal, Aleman, André, Baeken, Chris, et al. (2020) Evidence-based
624 guidelines on the therapeutic use of repetitive transcranial magnetic stimulation (rTMS): An
625 update (2014–2018). *Clinical Neurophysiology* **131**:2.
626 <https://doi.org/10.1016/j.clinph.2019.11.002>
- 627 Li, Zhe, Yin, Ming, Lyu, Xiao-Li, et al. (2016) Delayed effect of repetitive transcranial
628 magnetic stimulation (rTMS) on negative symptoms of schizophrenia: Findings from a
629 randomized controlled trial. *Psychiatry Research* **240**
630 <https://doi.org/10.1016/j.psychres.2016.04.046>
- 631 Li, Jiao, Seidlitz, Jakob, Suckling, John, et al. (2021) Cortical structural differences in major
632 depressive disorder correlate with cell type-specific transcriptional signatures. *Nature*
633 *Communications* **12**:1. <https://doi.org/10.1038/s41467-021-21943-5>
- 634 Li, Yongcong, Yang, Banghua, Ma, Jun, et al. (2024) Assessment of rTMS treatment effects
635 for methamphetamine addiction based on EEG functional connectivity. *Cognitive*
636 *Neurodynamics* <https://doi.org/10.1007/s11571-024-10097-x>
- 637 Liu, Meng, Ren-Li, Ren, Sun, Jingnan, et al. (2025) High-Frequency rTMS Improves Visual
638 Working Memory in Patients With aMCI: A Cognitive Neural Mechanism Study. *CNS*
639 *Neuroscience & Therapeutics* **31**:3. <https://doi.org/10.1111/cns.70301>
- 640 Margulies, Daniel S., Ghosh, Satrajit S., Goulas, Alexandros, et al. (2016) Situating the

641 default-mode network along a principal gradient of macroscale cortical organization.
642 *Proceedings of the National Academy of Sciences* **113**:44.
643 <https://doi.org/10.1073/pnas.1608282113>

644 Melnikov, Mikhail, Lopatina, Anna, Sviridova, Anastasiya, et al. (2025) The role of
645 neuroinflammation in schizophrenia: Focus on Th17 cells functions. *Asian Journal of*
646 *Psychiatry* **110** <https://doi.org/10.1016/j.ajp.2025.104629>

647 Menon, Vinod, and D'Esposito, Mark (2022) The role of PFC networks in cognitive control
648 and executive function. *Neuropsychopharmacology* **47**:1. [https://doi.org/10.1038/s41386-021-](https://doi.org/10.1038/s41386-021-01152-w)
649 [01152-w](https://doi.org/10.1038/s41386-021-01152-w)

650 Menon, Vinod, Palaniyappan, Lena, and Supekar, Kaustubh (2023) Integrative Brain
651 Network and Salience Models of Psychopathology and Cognitive Dysfunction in
652 Schizophrenia. *Biological Psychiatry* **94**:2. <https://doi.org/10.1016/j.biopsych.2022.09.029>

653 Mesulam, M. (1998) From sensation to cognition. *Brain* **121**:6.
654 <https://doi.org/10.1093/brain/121.6.1013>

655 Møller, Lisbeth Liliendal Valbjørn, Klip, Amira, and Sylow, Lykke (2019) Rho GTPases—
656 emerging regulators of glucose homeostasis and metabolic health. *Cells* **8**:5.
657 <https://doi.org/10.3390/cells8050434>

658 Morgan, Sarah E., Seidlitz, Jakob, Whitaker, Kirstie J., et al. (2019) Cortical patterning of
659 abnormal morphometric similarity in psychosis is associated with brain expression of
660 schizophrenia-related genes. *Proceedings of the National Academy of Sciences* **116**:19.
661 <https://doi.org/10.1073/pnas.1820754116>

662 Murray, John D, Bernacchia, Alberto, Freedman, David J, et al. (2014) A hierarchy of
663 intrinsic timescales across primate cortex. *Nature Neuroscience* **17**:12.
664 <https://doi.org/10.1038/nn.3862>

665 Olejarczyk, Elzbieta, Zuchowicz, Urszula, Wozniak-Kwasniewska, Agata, et al. (2020) The
666 Impact of Repetitive Transcranial Magnetic Stimulation on Functional Connectivity in Major
667 Depressive Disorder and Bipolar Disorder Evaluated by Directed Transfer Function and
668 Indices Based on Graph Theory. *International Journal of Neural Systems* **30**:04.
669 <https://doi.org/10.1142/S012906572050015X>

670 Owen, Michael J, Sawa, Akira, and Mortensen, Preben B (2016) Schizophrenia. *The Lancet*
671 **388**:10039. [https://doi.org/10.1016/S0140-6736\(15\)01121-6](https://doi.org/10.1016/S0140-6736(15)01121-6)

672 Paquola, Casey, Vos De Wael, Reinder, Wagstyl, Konrad, et al. (2019) Microstructural and
673 functional gradients are increasingly dissociated in transmodal cortices. (ed. H. Kennedy)
674 *PLOS Biology* **17**:5. <https://doi.org/10.1371/journal.pbio.3000284>

- 675 Park, Bo-yong, Bethlehem, Richard Ai, Paquola, Casey, et al. (2021) An expanding manifold
676 in transmodal regions characterizes adolescent reconfiguration of structural connectome
677 organization. *eLife* **10** <https://doi.org/10.7554/eLife.64694>
- 678 Postmes, L., Sno, H.N., Goedhart, S., et al. (2014) Schizophrenia as a self-disorder due to
679 perceptual incoherence. *Schizophrenia Research* **152**:1.
680 <https://doi.org/10.1016/j.schres.2013.07.027>
- 681 Ragland, J. Daniel, Gur, Ruben C., Valdez, Jeffrey, et al. (2004) Event-Related fMRI of
682 Frontotemporal Activity During Word Encoding and Recognition in Schizophrenia. *American*
683 *Journal of Psychiatry* **161**:6. <https://doi.org/10.1176/appi.ajp.161.6.1004>
- 684 Sale, Martin V., Mattingley, Jason B., Zalesky, Andrew, et al. (2015) Imaging human brain
685 networks to improve the clinical efficacy of non-invasive brain stimulation. *Neuroscience &*
686 *Biobehavioral Reviews* **57** <https://doi.org/10.1016/j.neubiorev.2015.09.010>
- 687 Schimmelpfennig, Jakub, Topczewski, Jan, Zajkowski, Wojciech, et al. (2023) The role of
688 the salience network in cognitive and affective deficits. *Frontiers in Human Neuroscience* **17**
689 <https://doi.org/10.3389/fnhum.2023.1133367>
- 690 Sciortino, Domenico, Pigoni, Alessandro, Delvecchio, Giuseppe, et al. (2021) Role of rTMS
691 in the treatment of cognitive impairments in Bipolar Disorder and Schizophrenia: a review of
692 Randomized Controlled Trials. *Journal of Affective Disorders* **280**
693 <https://doi.org/10.1016/j.jad.2020.11.001>
- 694 Sharbafshaaer, Mino, Cirillo, Giovanni, Esposito, Fabrizio, et al. (2024) Harnessing brain
695 plasticity: The therapeutic power of repetitive transcranial magnetic stimulation (rTMS) and
696 theta burst stimulation (TBS) in neurotransmitter modulation, receptor dynamics, and
697 neuroimaging for neurological innovations. *Biomedicines* **12**:11.
698 <https://doi.org/10.3390/biomedicines12112506>
- 699 Shi, Chuan, Yu, Xin, Cheung, Eric F.C., et al. (2014) Revisiting the therapeutic effect of
700 rTMS on negative symptoms in schizophrenia: A meta-analysis. *Psychiatry Research* **215**:3.
701 <https://doi.org/10.1016/j.psychres.2013.12.019>
- 702 Singh, Tarjinder, Poterba, Timothy, Curtis, David, et al. (2022) Rare coding variants in ten
703 genes confer substantial risk for schizophrenia. *Nature* **604**:7906.
704 <https://doi.org/10.1038/s41586-022-04556-w>
- 705 Sultana, Tajwar, Hasan, Muhammad Abul, Kang, Xiaojian, et al. (2023) Neural mechanisms
706 of emotional health in traumatic brain injury patients undergoing rTMS treatment. *Molecular*
707 *Psychiatry* **28**:12. <https://doi.org/10.1038/s41380-023-02159-z>
- 708 Sunkin, Susan M., Ng, Lydia, Lau, Chris, et al. (2012) Allen brain atlas: An integrated spatio-
709 temporal portal for exploring the central nervous system. *Nucleic Acids Research* **41**:D1.

- 710 <https://doi.org/10.1093/nar/gks1042>
- 711 Supekar, Kaustubh, Cai, Weidong, Krishnadas, Rajeev, et al. (2019) Dysregulated Brain
712 Dynamics in a Triple-Network Saliency Model of Schizophrenia and Its Relation to Psychosis.
713 *Biological Psychiatry* **85**:1. <https://doi.org/10.1016/j.biopsych.2018.07.020>
- 714 Tadin, Duje, Silvanto, Juha, Pascual-Leone, Alvaro, et al. (2011) Improved Motion
715 Perception and Impaired Spatial Suppression following Disruption of Cortical Area MT/V5.
716 *The Journal of Neuroscience*
- 717 Thomas Yeo, B. T., Krienen, Fenna M., Sepulcre, Jorge, et al. (2011) The organization of the
718 human cerebral cortex estimated by intrinsic functional connectivity. *Journal of*
719 *Neurophysiology* **106**:3. <https://doi.org/10.1152/jn.00338.2011>
- 720 Uddin, Lucina Q. (2015) Salience processing and insular cortical function and dysfunction.
721 *Nature Reviews Neuroscience* **16**:1. <https://doi.org/10.1038/nrn3857>
- 722 Urbaniak, Marta, Paczyńska, Małgorzata, Caramazza, Alfonso, et al. (2024) *Neural*
723 *Representation of Nouns and Verbs in Congenitally Blind and Sighted Individuals* n.p.:
724 Neuroscience <https://doi.org/10.1101/2024.04.14.589082>
- 725 Vafaii, Hadi, Mandino, Francesca, Desrosiers-Grégoire, Gabriel, et al. (2024) Multimodal
726 measures of spontaneous brain activity reveal both common and divergent patterns of cortical
727 functional organization. *Nature Communications* **15**:1. [https://doi.org/10.1038/s41467-023-](https://doi.org/10.1038/s41467-023-44363-z)
728 [44363-z](https://doi.org/10.1038/s41467-023-44363-z)
- 729 Wang, Luyao, Hu, Wenjing, Wang, Huanxin, et al. (2024) Different stimulation targets of
730 rTMS modulate specific triple-network and hippocampal-cortex functional connectivity. *Brain*
731 *Stimulation* **17**:6. <https://doi.org/10.1016/j.brs.2024.11.003>
- 732 Webler, Ryan D., Hamady, Carmen, Molnar, Chris, et al. (2020) Decreased interhemispheric
733 connectivity and increased cortical excitability in unmedicated schizophrenia: A prefrontal
734 interleaved TMS fMRI study. *Brain Stimulation* **13**:5.
735 <https://doi.org/10.1016/j.brs.2020.06.017>
- 736 Xi, Yi-Bin, Guo, Fan, Liu, Wen-Ming, et al. (2021) Triple network hypothesis-related
737 disrupted connections in schizophrenia: A spectral dynamic causal modeling analysis with
738 functional magnetic resonance imaging. *Schizophrenia Research* **233**
739 <https://doi.org/10.1016/j.schres.2021.06.024>
- 740 Xia, Mingrui, Liu, Jin, Mechelli, Andrea, et al. (2022) Connectome gradient dysfunction in
741 major depression and its association with gene expression profiles and treatment outcomes.
742 *Molecular Psychiatry* **27**:3. <https://doi.org/10.1038/s41380-022-01519-5>
- 743 Yan, Chao-Gan, Wang, Xin-Di, Zuo, Xi-Nian, et al. (2016) DPABI: Data Processing &

744 Analysis for (Resting-State) Brain Imaging. *Neuroinformatics* **14**:3.
745 <https://doi.org/10.1007/s12021-016-9299-4>

746 Zeng, Hongkui, Shen, Elaine H., Hohmann, John G., et al. (2012) Large-scale cellular-
747 resolution gene profiling in human neocortex reveals species-specific molecular signatures.
748 *Cell* **149**:2. <https://doi.org/10.1016/j.cell.2012.02.052>

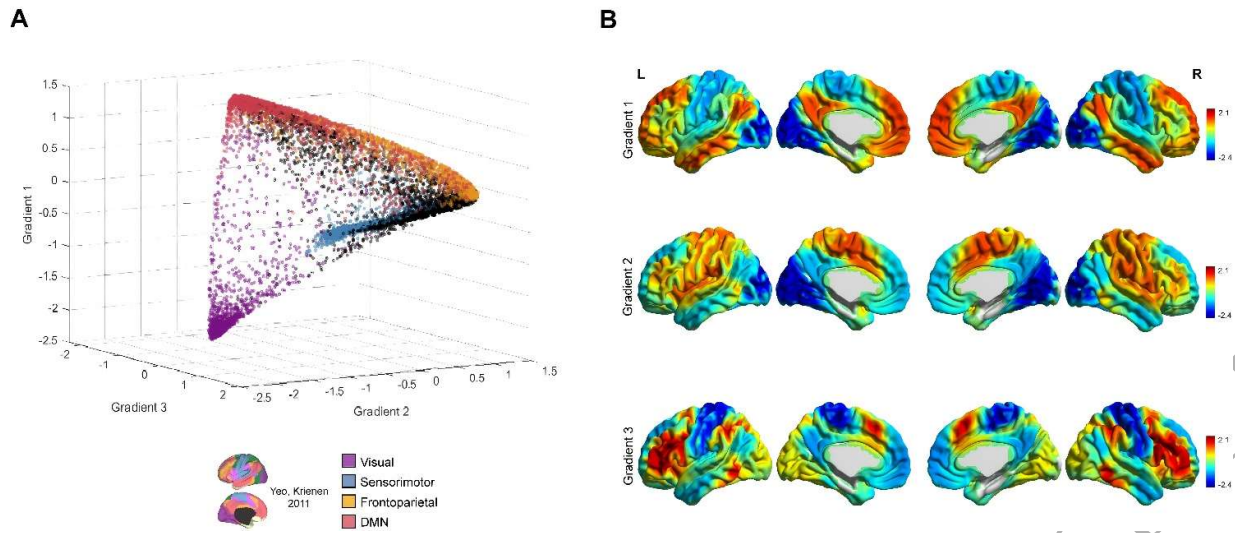
749 Zhang, Qirui, Li, Jiao, He, Yan, et al. (2023) Atypical functional connectivity hierarchy in
750 Rolandic epilepsy. *Communications Biology* **6**:1. <https://doi.org/10.1038/s42003-023-05075-8>

751 Zhao, Lei, Bo, Qijing, Zhang, Zhifang, et al. (2022) Altered Dynamic Functional
752 Connectivity in Early Psychosis Between the Salience Network and Visual Network.
753 *Neuroscience* **491** <https://doi.org/10.1016/j.neuroscience.2022.04.002>

754

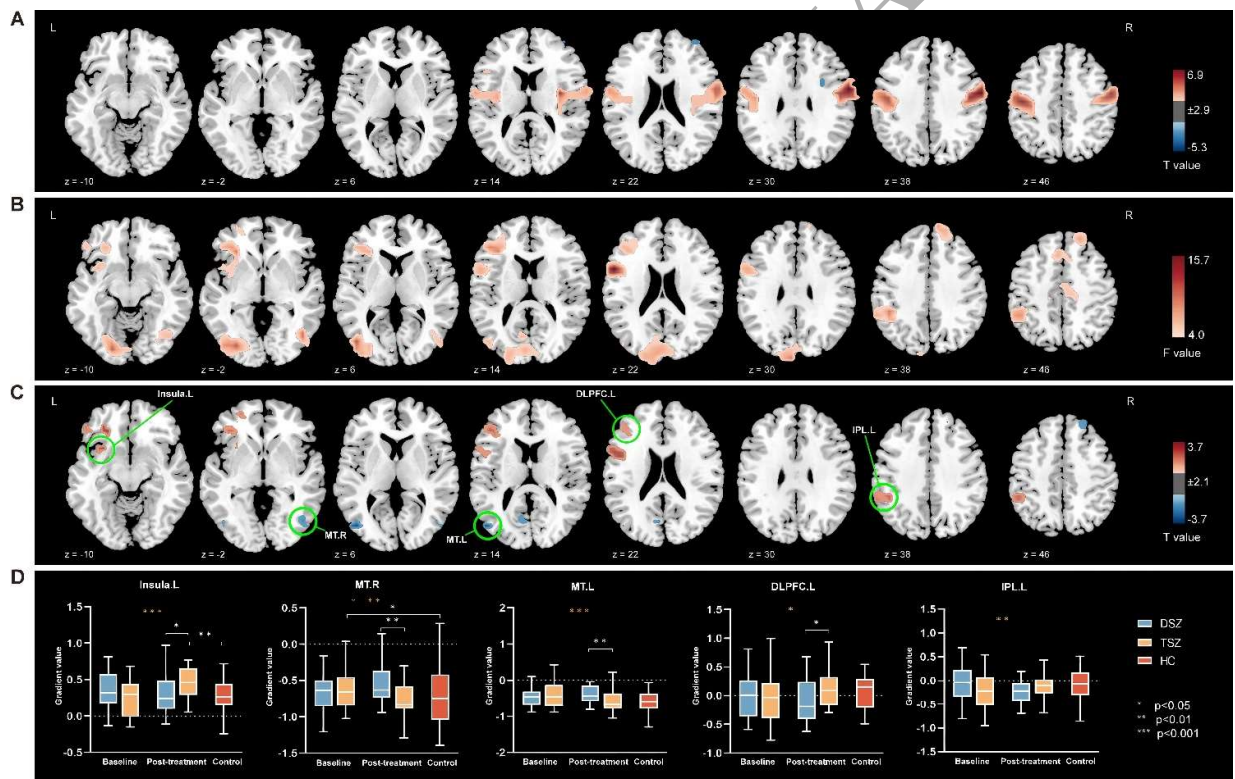
755

ORIGINAL UNEDITED MANUSCRIPT



757
758
759
760
761

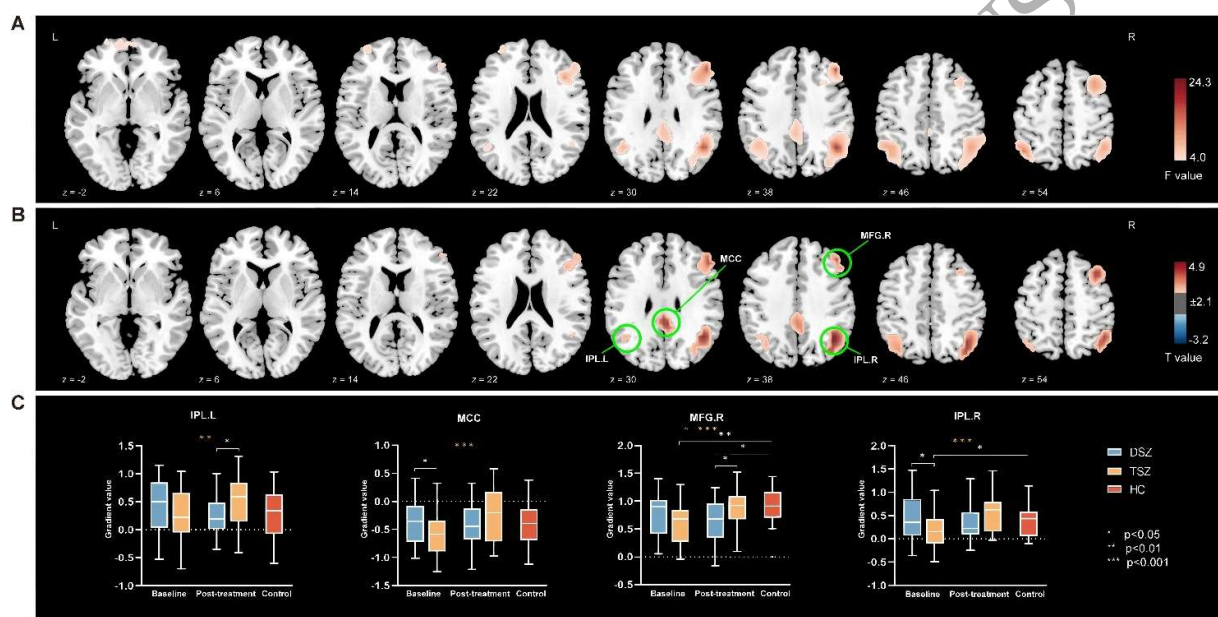
Fig.1. Gradients of HC group. **A)** Three-dimensional scatterplot of the first three gradient components from the HC group. **B)** The gradient map of the HC group. From top to bottom are the principal gradient (Gradient 1), the second gradient (Gradient 2), and the third gradient (Gradient 3).



762
763
764

Fig.2. Differences between schizophrenia & HC at baseline, rANOVA and post hoc test results of the principal gradient. **A)** Regions with significant differences between schizophrenia (DSZ & TSZ at

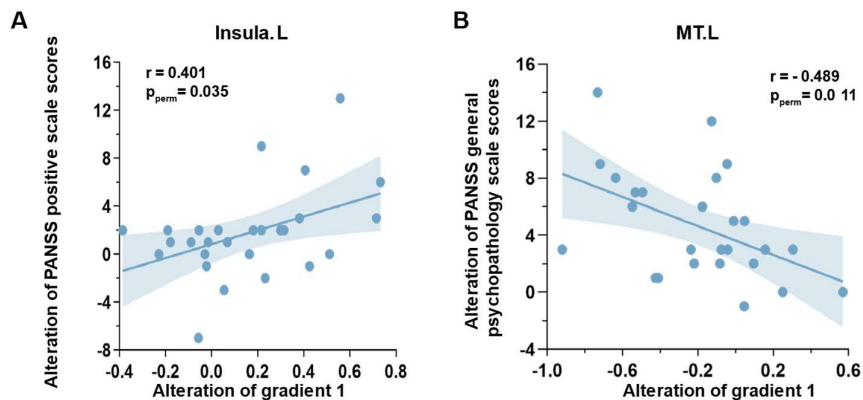
765 baseline) and HC group ($p_{FDR} < 0.05$). **B**) Regions showed a significant interaction between TMS
 766 treatment and time ($p < 0.05$). **C**) Regions showed significant differences in the post hoc paired t-test
 767 of the TSZ group (post-rTMS minus baseline, $p < 0.05$). **D**) Gradient intergroup differences within
 768 region of interest (ROI). From left to right are the regions of the Insula.L, the MT.R, the MT.L, the
 769 DLPFC.L, and IPL.L. The number of * represents the level of significance (* $p < 0.05$; ** $p < 0.01$;
 770 *** $p < 0.001$), and the color of * represents different tests (blue * represents paired t-test at baseline
 771 and after intervention in the DSZ group, orange * represent paired t-tests at baseline and after
 772 intervention in the TSZ group, and white * represents two-sample t-tests). MT: middle temporal visual
 773 area, DLPFC: the dorsolateral prefrontal cortex, MFG: middle frontal gyrus, IPL: inferior parietal
 774 lobule.
 775



776
 777 **Fig.3.** rANOVA and post hoc results of gradient 3. **A**) Regions showed a significant interaction
 778 between TMS treatment and time ($p < 0.05$). **B**) Regions showed significant differences in the post hoc
 779 paired t-test of the TSZ group (post-rTMS minus baseline, $p < 0.05$). **C**) Gradient intergroup
 780 differences within ROI. From left to right are the regions of the IPL.L, the MCC, the MFG.R, and the
 781 IPL.R. The number of * represents the level of significance (* $p < 0.05$; ** $p < 0.01$; *** $p < 0.001$), and
 782 the color of * represents different tests (blue * represents paired t-test at baseline and after intervention
 783 in the DSZ group, orange * represents paired t-test at baseline and after intervention in the TSZ group,

784 and white * represents two-sample t-tests). MFG: middle frontal gyrus, IPL: inferior parietal lobule,
 785 MCC: middle cingulate cortex.

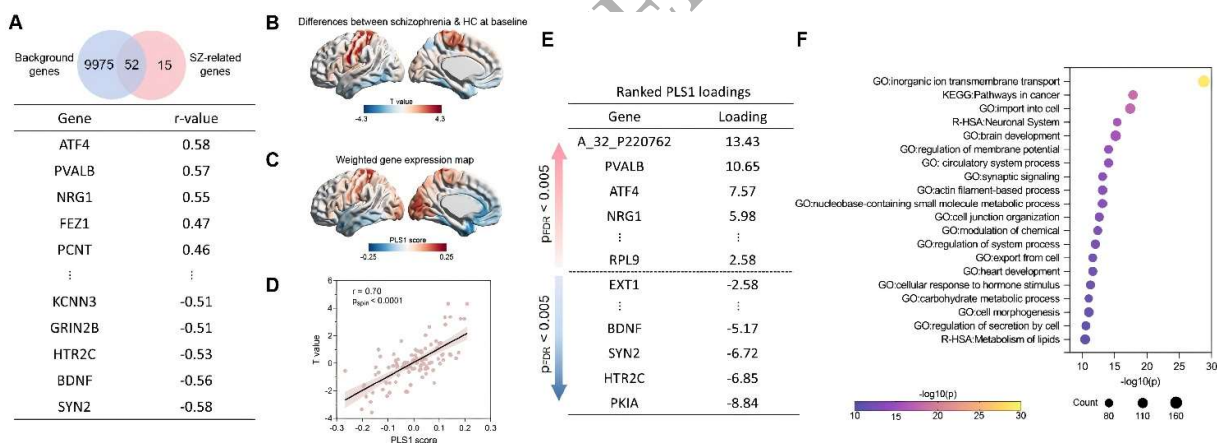
786



787

788 **Fig.4. A)** The alteration of principal gradient (post minus baseline) in the left insula was associated
 789 positively with the alteration of PANSS positive scale scores (baseline minus post) with positive values
 790 representing the improvement of symptoms. **B)** The alteration of the principal gradient (post minus
 791 baseline) in left MT was associated negatively with the alteration of PANSS general psychopathology
 792 scale scores (baseline minus post). Significance was assessed using permutation testing (n = 5,000).
 793 MT: middle temporal visual area.

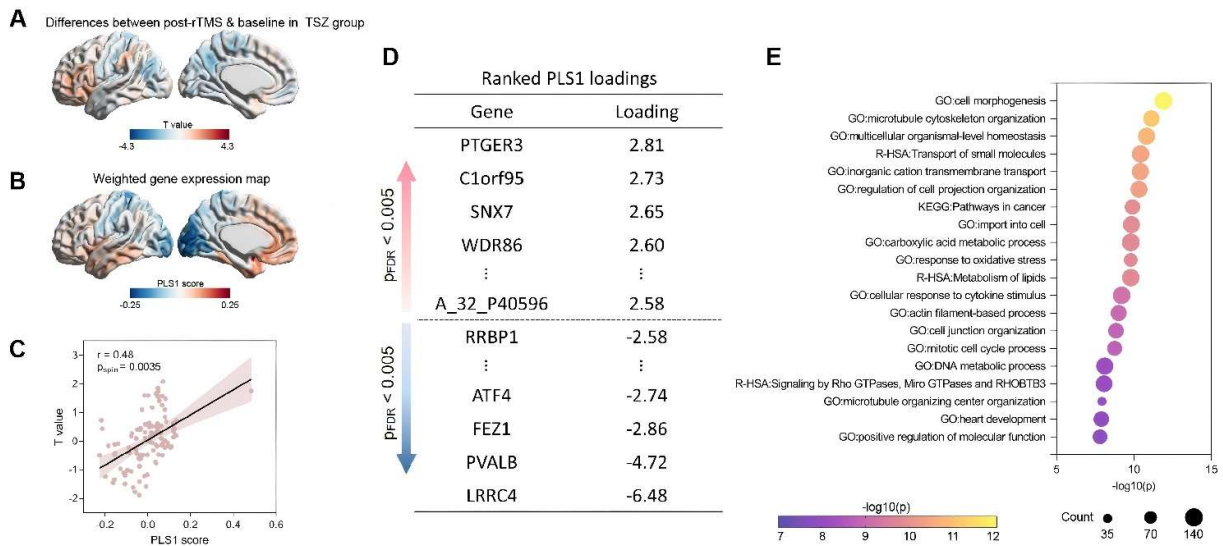
794



795

796 **Fig.5.** Schizophrenia-associated genetic profiles related to principal gradient differences. **A)**
 797 Schizophrenia-associated genes from in situ hybridization (ISH) overlapped with 10,027 background
 798 genes and were correlated with alteration of principal gradient in schizophrenia. **B)** Principal gradient
 799 differences between schizophrenia (DSZ & TSZ at baseline) and HC group. **C)** Cortical map of

800 regional PLS1 scores. **D)** Scatterplot showing the relationship between regional PLS1 scores and
 801 principal gradient differences. **E)** Ranked PLS1 scores. **F)** Functional enrichment ontology terms
 802 related to the alteration of principal gradient in the PLS+ ($Z > 5$) and PLS- ($Z < -5$) gene list (all p_{FDR}
 803 < 0.005). GO, gene ontology. KEGG, Kyoto Encyclopedia of Genes and Genomes.
 804



805
 806 **Fig.6.** Genetic profiles related to the changes of principal gradient induced by rTMS. **A)** Principal
 807 gradient differences of TSZ group (post-rTMS minus baseline). **B)** Cortical map of regional PLS1
 808 scores. **C)** Scatterplot illustrating the correlation between regional PLS1 scores and rTMS-induced
 809 gradient differences. **D)** Ranked PLS1 scores. **E)** Functional enrichment ontology terms related to the
 810 rTMS-induced alteration of principal gradient in the PLS+ and PLS- gene list (all $p_{FDR} < 0.005$). GO,
 811 gene ontology. KEGG, Kyoto Encyclopedia of Genes and Genomes.
 812
 813
 814